LONG-LIFE CORES
WITH SMALL BURNUP REACTIVITY SWING

E. Greenspan, H. Shimada and K. Wang
Department of Nuclear Engineering
University of California
Berkeley, CA 94720
gehud@nuc.berkeley.edu

ABSTRACT

The neutronic feasibility of designing small and simple lead cooled and reflected cores to operate up to the metallurgical limit with nearly zero burnup reactivity swing is investigated. These cores are loaded with uniform composition fuel, they have no blanket assemblies, and they operate without any fuel shuffling. The design domain has been defined for such cores that can deliver 125 to 250 MW_{th}. The radiation damage to the clad limits the average linear heat-rate of a core that is to operate for 15 effective full power years to 80 w/cm, when the fuel is 1 cm in diameter. The corresponding peak burnup of these cores is approximately 100 GWD/tHM. The dependence of selected neutronic characteristics of the nearly zero burnup reactivity swing Pb-cooled cores on selected core design variables was established.

1. INTRODUCTION

If a core could be designed to have a uniform fuel composition and to maintain, without any fuel handling, a nearly constant k_{eff} up to the radiation damage limit, it will be very attractive for the following reasons: (a) Good proliferation resistance. (b) Simplified control. (c) Improved safety (d) Reduced O&M costs. (e) Improved availability.

For these reasons one of the design goals set for the recently conceived[1] Encapsulated Nuclear Heat Source (ENHS) reactor core was to have a 15 years life with nearly zero burnup reactivity swing. In a preliminary study we illustrated[2,3] that this might be feasible in small Pb-cooled and reflected cores that are fueled with either Pu-U-Zr($10^{w}/_{o}$) or U-Zr($10^{w}/_{o}$).

The primary purpose of the present work is to establish the range of core design variables that enable operating the core for 15 Effective Full Power Years (EFPY) with nearly zero reactivity swing without any fuel handling and without exceeding the radiation damage related constraints. The study focuses on lead-cooled cores that have uniform initial composition and do not have any blanket elements or special reflector elements; the lead that surrounds the core provides also for neutron reflection. Another purpose of this work is to explore the neutronic characteristics of

the nearly zero burnup reactivity swing Pb-cooled cores and the systematics of the dependence of these characteristics on the selected core design variables.

Even though Pb is the only coolant specifically considered in this work, all the reported results also apply to Pb-Bi coolant.

In Section 2 we briefly review prior art in the design of close to zero burnup reactivity swing cores. The ENHS core model considered in this work is described in Section 3. Section 4 describes the computational method along with the set of assumptions used. Section 5 describes the dependence of selected neutronic characteristics on core design variables. The design domain identified for nearly zero burnup reactivity swing cores for 15 EFPY is summarized in Section 6. Section 7 discusses the implications of certain of the approximation used in this work. Conclusions are presented in Section 8.

2. PRIOR ART

Orlov and Adamov[4,5] appears to be the first to suggest that Pb-cooled reactors can be designed to have a nearly zero burnup reactivity swing. One of their reactor design goals was to restrict the available excess reactivity to less than one dollar. To achieve this they have a relatively often refueling – once every year. The fuel residence time in the core is 5 years. The peak discharge burnup is between 6 to 12 percent. The average linear heat rate varies between 210 and 320 w/cm.

Sekimoto[6,7] et al. designed small Pb-cooled cores using either metallic alloy or nitride fuel. They considered three-zone cores that are to operate for more than 10 years without refueling or fuel shuffling, while maintaining burnup reactivity swings to less than 0.1% $\Delta k/k$. Other restrictions included a negative whole core void coefficient of reactivity over all of the burnup period.

C. Rubbia[8] et al. designed a Pb-cooled slightly subcritical core that is to be driven by an intense accelerator neutron source. One of their, so called, Energy Amplifier design features is a nearly burnup independent k_{eff} value.

A couple of features that are common to all these core designs are (a) fast spectrum, and (b) breeding ratio that is slightly above unity. The second feature implies that the fissile fuel content is very slightly increasing with burnup. The first feature implies that the accumulation of fission products (FP) does not significantly impair the neutron balance; a slight buildup of fissile fuel content can compensate for the negative reactivity effect of the FP.

The notion that any combination of fertile fuel, coolant, structural materials and possibly moderator has its equilibrium fissile fuel content was established many years ago; see for example reference 9. That reference considered lattices using U-Pu oxide fuel that are cooled by regular or heavy water. It showed that the smaller is the water-to-fuel volume ratio, the higher becomes the equilibrium fissile fuel contents. For the k_∞ corresponding to an equilibrium fissile fuel content to exceed unity, the neutron spectrum need be hard. This implies using a very small water-to-fuel volume ratio. The added advantage of a hard spectrum is small neutron absorption

probability by the accumulating FP. By designing the core to slightly breed, it is possible to compensate for the poisoning effect of the FP so as to maintain k_∞ practically burnup independent.

3. THE ENHS CORE MODEL

The ENHS model used for the neutronic analysis is described in figure 1 and in table I. The layout of the core and adjacent components are similar to those of the 4S reactor[10,11]. The system considered in this work differs from that of the 4S reactor in the coolant type, the composition of the radial reflector and shield, and in the core dimensions.

The core consists of fuel assemblies having 217 rods in a hexagonal array. The central assembly site is reserved for a safety rod assembly. During reactor operation this central site is filled with Pb. There are no control rods. The fine tuning of reactivity is done by axial movement of the radial reflector. Also, there are no blanket assemblies and no reflector assemblies. The Pb that surrounds the core serves as the reflector. All the fuel rods are of a uniform composition. Each fuel rod has a fission gas plenum above the fuel section; the plenum length is taken to be 75% of the fuel section length. The fuel is a metallic alloy of U-Pu with 10 weight % Zr; its density is assumed to be 75% of the nominal density. The uranium is depleted to 0.2 $^{w}/_{o}$ ^{235}U and the Pu initial composition is typical to that from LWR spent fuel: the weight % of the isotopes 239, 240, 241 and 242 is, respectively, 67.2, 21.7, 6.4, and 4.7. The clad is represented by stainless steel having 64.8 $^{w}/_{o}$ Fe, 17 $^{w}/_{o}$ Cr, 14 $^{w}/_{o}$ Ni, 2.8 $^{w}/_{o}$ Mo and 1.5 $^{w}/_{o}$ Mn. In reality, lower Ni contents steel such as HT-9 will be used with the Pb coolant. The same SS composition is assumed for all the structural components modeled for the neutronic analysis.

The central absorber (denoted in figure 1 as the “safety rod region”) is securely latched inside the core as long as the coolant temperature is below 350C. This is accomplished with an electromagnetic latch that connects the central absorber to its withdrawal mechanism; the latch does not engage until its temperature exceeds 350C. After the central absorber is withdrawn, all the reactivity control is done with the radial reflector assembly. That is, the reflector is to compensate for the reactivity swing due to temperature increase above 350C and due to fuel burnup. The nominal core inlet, outlet and average temperatures are assumed to be 420C, 540C and 480C.

The reflector assembly includes a voided container that is 15 cm thick and as long as the fuel section in the core. The minimum reactivity worth of the reflector is obtained when the cavity level coincides with the fuel level in the core. The maximum reactivity worth is obtained when the cavity is all below (or above) the core, so that Pb surrounds the core. Additional information on the ENHS design can be found in reference 12.

4. COMPUTATIONAL METHOD AND ASSUMPTIONS

The calculations are done using MCNP[13] and ORIGEN2[14] managed by the MOCUP code[15]. MCNP calculates k_{eff}, zone-wise fluxes, relative power and effective one group averaged cross

sections for use in ORIGEN2. ORIGEN2 calculates the change in the isotopic composition as a function of time. Most of the burnup dependent results reported below were obtained by performing the MCNP calculations once every year of reactor full power operation, treating the core as a single zone. That is, the isotopic composition across the core is uniform from beginning-of-life (BOL) to end-of-life (EOL). The effect of finer burnup time steps and of space-dependent depletion is discussed in Section 7.

Tables II and III define the cross sections used for the MCNP calculations. Not all the FP with non-negligible absorption probability are accounted for. In Section 7 we will estimate the effect of the FP not accounted for. MCNP generated effective one-group cross sections of all these isotopes are used for the ORIGEN2 burnup analysis. For isotopes not included in MCNP analysis, ORIGEN2 uses cross sections from its pre-processed libraries. For the present study we used ORIGEN2 libraries number 312 for actinides and 313 for FP; they were both intended for LMFBR analysis and were generated using a hard neutron spectrum. In Section 7 we'll check the sensitivity of the results to the ORIGEN2 library selection.

The design variables of this study are the core height, lattice pitch-to-diameter ratio (p/d), initial plutonium weight percent, total core thermal power and average linear heat rate, q'_{av}. Three power levels and two q'_{av} values are considered: 62.5, 125 and 250 MW_{th}, and 80 and 120 w/cm. The fuel rod diameter and clad thickness were fixed at 1 cm and 0.1 cm, respectively.

The core design is subjected to a couple of constraints: the peak fuel burnup should not exceed 150 GWD/tHM, and the peak fluence of E > 0.1 MeV neutrons should not exceed $4x10^{23}$ n/cm^2. Other restraints on the core design are: maximum fuel length is 4 m and minimum p/d is 1.15.

The critical Pu loading – the Pu weight % to be loaded in the fuel for a given core, is determined so that the k_{eff} value for a cold and clean core will be 0.994. This provides a margin to criticality of 1.3 dollars, as the average delayed neutron fraction for a typical Pb-cooled core, estimated in table IV, is 0.0046. This approach is conservative; in reality it is not acceptable to get the core critical when its temperature is below the coolant melting temperature. As described in Section 3, the ENHS is designed to be at shutdown conditions as long as its coolant temperature is below 350C. A practical design approach would be designing the Pu loading to provide a k_{eff} of ~0.995 when the core is at 350C.

The Initial Conversion Ratio (ICR) considered in this work is the conventional definition: the ratio of neutron capture rate in ^{238}U and ^{240}Pu to neutron absorption rate in ^{235}U, ^{239}Pu and ^{241}Pu. It turns out that in the hard spectrum of Pb cooled reactors, the even fuel isotopes contribution to fission is not negligible. For example, table IV shows that the ^{238}U fission rate is second to that of ^{239}Pu; it is twice as large as that of ^{241}Pu. Also shown in table IV is that the BOL fission rate of ^{240}Pu is ~60% of that of ^{241}Pu. Hence, the conventional ICR definition used in this work is not a good characterization of the rate of change of the fuel quality.

The flux amplitude used for burnup analysis in ORIGEN2 is obtained from the MCNP results through use of the MOCUP "flux normalization factor" fmt. It is calculated as follows: $\mathbf{fmt\ (1/s) = \nu\ P\ /\ (1.602\ x\ 10^{-19} x\ k_{eff}\ x\ R_a)}$, where ν is the average number of neutrons per fission, P is the

reactor thermal power in MW, and R_a is the average recoverable energy, in MeV, per fission. A value of 204.5 MeV/fission recommended by one of the MOCUP developers[16] was used for R_a throughout this study. Using MCNP BOL fission probability data and isotope dependent recoverable energy data we are estimating, in table V, the recoverable energy for a typical Pb cooled reactor considered in this work to be 209.2 MeV/fission. This implies that the actual power level can be approximately 2% higher than the one assumed for the present analysis.

5. NEUTRONIC CHARACTERISTICS SYSTEMATICS

A parametric study has been performed with the aim of establishing the dependence of various system characteristics on four core design variables: core height, lattice p/d ratio, core power level and average linear heat rate of the fuel rods. The trends obtained for 250 MW_{th} cores that are designed to have a q'_{av} value of 120 w/cm are shown in figures 2 through 12. Supplementary results are provided in tables VI and VII. Following are several observations concerning the systematics of selected neutronic characteristics:

1. The critical Pu concentration increases (Figure 2) and, correspondingly, the ICR decreases (Figure 3) as p/d increases. This is due to an increase of the absorption probability in Pb (Figure 7), to enhancement of the leakage probability (Figure 4) as well as to spectrum softening as p/d increases. In general, the higher is p/d for a given core height, the larger becomes the core diameter (tending to reduce the leakage probability) but the longer becomes the mean distance the neutron travel until it is absorbed (tending to increase the leakage probability). The latter effect is the dominant, as can be deduced from the one-group diffusion theory expression for the non-leakage probability of bare cores: $\mathbf{P_{NL} = [1+ B^2L^2]^{-1}}$. $\mathbf{B^2}$ is the geometric buckling and $\mathbf{L^2}$ is the diffusion area. The radial buckling $\mathbf{B_r^2 \propto R^{-2}}$ whereas $\mathbf{L^2 = D/\Sigma_a}$. The diffusion coefficient **D** is, to first order, independent of p/d. $\mathbf{\Sigma_a}$ on the other hand, is nearly proportional to the HM concentration which is $\mathbf{\propto R^{-2}}$. Hence, $\mathbf{L^2 \propto R^2}$ and $\mathbf{D_r^2L^2}$ is, to first approximation, independent of **R**. The axial buckling, $\mathbf{B_a^2}$ is independent of **R** so that $\mathbf{B_a^2L^2 \propto R^2 \propto (p/d)^2}$.
2. The 2 m high cores require the lowest Pu concentration and offer the highest ICR whereas the 4 m high cores require the highest Pu concentration and have the lowest ICR (Figures 2 and 3). This is well correlated with the leakage probability of these cores (Figure 4). Of the three core heights considered, the 2 m high cores are the least leaky, as they have the smallest ratio of surface area to volume. The 1 m high core is the most sensitive to p/d as far as the critical Pu concentration and ICR are concerned. Figure 4 shows that these trends are correlated with the leakage probability dependence on p/d. The dominant leakage in the pancake shaped cores is in the axial direction. And as shown in "point 1" above, the axial leakage is the leakage component that increases with p/d.
3. The reactivity worth of the reflector is sensitive to the core height but not to p/d (Figure 5). This indicates that the radial leakage probability is closely independent of p/d. Combining the trends provided by figures 4 and 5 it appears that p/d affects, primarily, the axial leakage probability. These trends can be anticipated based on simple one-group diffusion theory analysis carried out in "point 1" above. The taller the core, the higher is the reflector reactivity worth. This expected trend is correlated with the tendency of the radial leakage probability to increase with a reduction in the core diameter, i.e., with an increase in the core height. The findings of figure 5 may have important practical implications: pancake shaped

cores may not have large enough reflector reactivity worth to compensate for the temperature and burnup reactivity swings.

4. The void reactivity worth is positive throughout the range considered for the core design variables. It increases with p/d and is not so sensitive to the core height (Figure 6). Voiding the core affects k_{eff} via three phenomena: spectrum hardening (positive effect), reduced parasitic absorption by Pb (positive), and enhanced leakage probability (negative). The reactivity worth reported in figure 6 corresponds to replacement of Pb by void throughout the core volume, but not outside the core. Creation of such a void is practically impossible; the boiling temperature of Pb is 2022K, significantly higher than the melting temperature of SS and of the metallic fuel. We can think of no scenario that can bring the Pb to even close to its boiling temperature. Even if there is a scenario that could have caused the Pb temperature to keep increasing, the clad and fuel will melt and dissolve in the Pb before the Pb will get to its boiling point. Dissolution of the fuel in the Pb will result in a large reactivity loss that is likely to be followed by reactor shutdown. The only conceivable voiding mechanism we could think of is a leakage of Pb from the reactor vessel. This mode of voiding turns out to have a negative reactivity effect, as illustrated in table VIII. This illustration pertains to 2 m high cores. The negative effect is due to the enhanced leakage probability that more than compensates for the positive effects of spectrum hardening and reduction in the parasitic neutron absorption probability. The couple of positive values in table VIII are probably due to statistical uncertainties in the Monte Carlo calculations.
5. Table IX gives the hot-to-cold reactivity swing for selected cores. This reactivity swing consists of four components: (a) Pb density change. (b) Fuel axial expansion. (c) Radial expansion of core support structure. (d) Doppler effect. All these components are the difference in k_{eff} values between the cold temperature and 700C or 480C for, respectively, the Doppler effect or the rest of the effects. Two "cold" temperatures are considered: (a) Room temperature, taken to be 20C, and (b) 350C – the temperature above which it is possible to withdraw the central absorber rod; at lower temperatures it is impossible to bring the reactor to criticality. The Pb density is assumed to be 11.368 g/cm^3 at 20C and **11.072-1.2[T(K)-273]** g/cm^3 for T in between 673K and 973K. The coefficient of linear expansion was assumed to be 1.78×10^{-5} K^{-1} for the core support structure and 1.9×10^{-5} K^{-1} for the fuel. Upon expansion, the core is assumed to maintain a cylindrical shape; that is, we do not account for enhanced radial expansion of the upper part of the core that is the hottest.
6. The effect of the core power level on several of the characteristics considered above is illustrated in figures 8 through 12. The results pertain to 4 m high cores operating at a q'_{av} of 120 w/cm. The number of fuel rods of these cores is proportional to the power level. For a given p/d, the core diameter is closely proportional to the square root of the power level. That is, the lowest power cores have the largest radial leakage probability, making their reflector reactivity worth the highest (Figure 12) and their void reactivity effect the smallest (Figure 11).
7. The effect of the average fuel linear heat rate on the neutronic characteristics is inversely proportional to the effect of the core power level; the larger the linear heat rate, the smaller is the total length of fuel rods needed for generating a given power level. For a given core height, the core diameter is closely inversely proportional to q'_{av}. Thus, the dimensions of a core for 250 MW_{th} having q'_{av} of 120 w/cm will be identical to the dimensions of a core for

125 MW_{th} with q'_{av} of 60 w/cm when both have the same p/d ratio. Cores designed to deliver 125 MW_{th} with q'_{av} of 80 w/cm will be only slightly smaller.

8. It is also found that the power density shape is not sensitive to the core dimensions. Typically, the peak-to-average power density is between 1.8 to 2.0.
9. Figures 13 and 14 illustrate the sensitivity of the burnup reactivity swing to the p/d ratio. The fluctuations are stochastic in nature; they are due to the use of MCNP for calculating k_{eff} and, even more so, for generating the effective one-group cross sections for the burnup analysis. It is observed that for a core of a given power, height and q'_{av}, there exists a p/d ratio for which k_{eff} can stay practically constant for many years of operation. This happens, for example, for 13 years of effective full power operation of the core for 250 MW_{th}, 4 m, 120 w/cm core of figure 13 having a p/d ratio of 1.30. Designing a similar core to have a slightly larger p/d ratio will lead to k_{eff} that is monotonously declining with operation time. This is illustrated by the p/d = 1.375 core of figure 13 and by the p/d = 1.60 core of figure 14. The burnup reactivity swing of the last two cores over 15 effective full power years (EFPY) is, respectively, approximately 1.5% and 0.8%. This reactivity swing can be compensated by an automated constant movement of the radial reflector at an infinitesimally small speed – on the order of the 1 mm/day proposed for the 4S reactor[7,8]. When p/d is smaller than a certain value, k_{eff} will tend to initially increase with burnup, as illustrated for the p/d = 1.525 case of figure 14.
10. The evolution of the concentration of fuel isotopes with EFPY of operation is illustrated in figures 15 and 16. The data in these figures is normalized to the BOL HM inventory. It is observed that the inventory of the two most abundant Pu isotopes – 239 and 240 slightly increases for the first 15 EFPY of operation, while that of the higher Pu isotopes and of ^{235}U is dropping. Comparing figures 15 and 16 it is observed that, in the p/d range considered, the relative change in the fuel isotope concentration is not sensitive to the core p/d ratio.

6. DESIGN DOMAIN FOR ZERO BURNUP REACTIVITY SWING

Guided by the above information we proceeded to define the combination of core design variables that will yield nearly zero burnup reactivity swing for, at least, 15 EFPY. Figures 17 and 18 define the combination of core height and p/d ratio that have nearly zero burnup reactivity swing for 15 years of full power operation. The two curved plots shown in each of the figures each represents a family of cores for a given total power output – 125 MW_{th} for the left hand plot and 250 MW_{th} for the right-hand plot. The core diameter is uniquely defined by the core height, p/d value, fuel rod outer diameter (1.2 cm, in the present study), q'_{av} (80 or 120 w/cm) and core thermal power. The bottom boundary is the criticality constraint. The dashed line saying "Minimum critical height for dk_{eff} = 1.0% temperature reactivity loss" defines the minimum height of cores whose reflector reactivity worth is 1.6%. As the unreflected cores of figures 17 and 18 are designed to have k_{eff} = 0.994 when at room temperature, the room temperature k_{eff} of the reflected cores is 1.01. The 1% excess reactivity is to compensate for the burnup reactivity swing. The dotted line for 0.28% of dk_{eff} due to hot-to-cold temperature swing corresponds to 350C as the cold temperature for the core design. This line provides the most realistic bound for the core design domain.

Of the family of acceptable cores defined by figure 17 , the 2 m high core having a p/d of 1.3 appears attractive. This core enables designing relatively compact ENHS modules, as illustrated

by Case 9.2.5 of table 2 of reference 12. Figure 19 shows the burnup reactivity swing of this core. k_{eff} varies by not more than ~0.5% over 30 years of EFPY of operation! The fluctuations in k_{eff} are stochastic; they are due to the use of the MCNP Monte-Carlo code for calculating k_{eff}. The optimal k_{eff} versus burnup profile may be somewhat different from that of figure 19; either flatter or having a slightly negative slop. The reactivity loss will be compensated, in the latter case, by a constant automatic creeping movement of the reflector.

The cores defined in figure 17 and 18 (by the two curved lines) all reach the peak fast neutron fluence constraint after ~15 EFPY. For a 1 cm fuel diameter, this constraint limits the linear heat rate to 80 w/cm. The resulting peak burnup is ~105 GWD/tHM. Had 10 EFPY been acceptable life for the ENHS, its core could have been designed for an average linear heat rate of 120 w/cm.

7. DISCUSSION

A number of approximations were used in the calculations the results from which were reported above. In the following we shall estimate the significance of these approximations.

7.1 UNIFORM HOMOGENEOUS CYLINDRICAL CORE MODEL

The core consists of hexagonal heterogeneous unit cells assembled into fuel assemblies. A core made of hexagonal fuel assemblies can not be exactly cylindrical. The question addressed is what error is introduced by volume averaging the heterogeneous unit cell and by cylindericizing the core. Both effects were found negligible.

7.2 SINGLE ZONE BURNUP ANALYSIS

All the burnup dependent results reported above were obtained from a single zone analysis; that is, ignoring space dependent composition. Figure 20 compares k_{eff} evolution as calculated for the same core using two approaches: (a) A 10 zone analysis: the core is divided into ten equal volume radial zones. The burnup of each of the 10 zones is analyzed separately. (b) A single zone analysis. This comparison is done for a 4 m high 250 MW_{th} core having p/d = 1.15 and q'_{av} = 120 w/cm. It is observed that the single zone analysis tends to overestimate the value of k_{eff} for long operating times. Figure 21 shows that the buildup of ^{239}Pu in the outermost zone of the 10 zone core is significantly more pronounced than its buildup in the inner zones. The enhanced buildup in the outer zone is due to the effect of the radial reflector. As the importance of fission neutrons born near the core boundary is smaller than the importance of fission neutrons born closer to the core center, the non-uniform buildup of Pu is responsible for a lower k_{eff}. The implication of this finding is that the p/d value for the real core will have to be slightly smaller than the p/d value found optimal using a single zone analysis. The k_{eff} evolution of the real core can be as flat as calculated using the single-zone approximation.

7.3 BURNUP TIME STEPS

All the burnup analysis reported so far made one MCNP calculation every one EFPY. If the neutron spectrum in the core varies significantly during one year, MCNP should recalculate the

effective one-group transmutation cross sections more frequently. Figure 22 compares the k_{eff} evolution with operation time as calculated using two frequencies for MCNP calculations: 0.1 and 1 year per calculation. No difference is observed in the general trend. It is concluded that once a year is a sufficient frequency for MCNP calculations of our Pb cooled systems.

7.4 UNACCOUNTED FOR FISSION PRODUCTS

Forty seven FP are accounted for in the MCNP calculations; they are listed in table III. MCNP cross sections for other FP were not available to us. Using the ORIGEN2 FP data we have estimated that the FP used in the MCNP calculations account for 73% of the absorption by all the FP. We also estimated that the reactivity effect of the FP not accounted for in MCNP is, approximately, 1% after 15 EFPY. This small, but non-negligible effect can be compensated for by a slight reduction in the p/d value.

7.5 SENSITIVITY TO FISSION PRODUCTS LIBRARY

A number of FP libraries for LMFBR are found in the ORIGEN2 code package. Libraries number 312 and 313 were used for the calculations reported upon above. One run was done using libraries number 372 and 373. Figure 23 compares the evolution of k_{eff} as calculated using the two sets of libraries. It is observed that the results are insensitive to the libraries used.

CONCLUSIONS

It is concluded that small and simple lead cooled and reflected cores that are loaded with uniform composition fuel and without blanket assemblies can be designed to operate without any fuel handling up to the metallurgical limit with nearly zero burnup reactivity swing. The range of design variables of such cores has been identified. The dependence of selected neutronic characteristics of the nearly zero burnup reactivity swing cores on core design variables was established.

ACKNOWLEDGMENT

This work was supported by the DOE NERI program under contract No. DE-FG03-99SF21889

REFERENCES

1. E. Greenspan and D.C. Wade, “Encapsulated Nuclear Reactor Heat Source Module,” Transactions Am. Nucl. Soc., 80, 197-199 (1999).

2. H. Shimada, E. Greenspan, N. Stone and S. Wang, “Long-Life Lead-Cooled Core Fueled with Enriched Uranium,” Transactions Am. Nucl. Soc., 80, 199-200 (1999).

3. A.S. Boloori et al., “Once-for-Life Fueled, Highly-Modular, Simple, Super-Safe, Pb-Cooled Reactors”, Proc. Int. Conf. On Advances in Fuel Cycle, GLOBAL’99, Jackson Hole,

Wyoming, Aug. 29-Sept. 3, 1999. See also in Transactions Am. Nucl. Soc., 80, 200-201 (1999).

4. V.V. Orlov et al., "Lead-Cooled Reactor Core, its Characteristics and Features," Int. Top. Mtg. On Advanced Reactor Safety, ARS 94, Pittsburgh, PA, April 17-21, 1994.

5. E.O. Adamov, V.V. Orlov, A.I. Filin, V.N. Leonov, A.G. Sila-Novitski, V.S. Smirnov, and V.S. Tsikunov, "The Next Generation of Fast Reactors," Nuclear Engineering and Design, Vol. 173, pp. 143-150 (1997).

6. H. Sekimoto and Z. Su'ud, "Design Study of Lead and Lead-Bismuth-Cooled Small Long-Life Nuclear Power Reactors Using Metallic and Nitride Fuels," Nuclear Technology, Vol. 109, pp. 307-313, 1995.

7. Z. Su'ud and H. Sekimoto, "Design and Safety Aspect of Lead and Lead-Bismuth Cooled Long-Life Small Safe Fast Reactors for Various Core Configurations," Journal of Nuclear Science and Technology, Vol. 32, pp. 8-19, 1995.

8. C. Rubbia et al., "Conceptual Design of a Fast Neutron Operated High Power Energy Amplifier," European Organization for Nuclear Research Report CERN/AT/95-44 (ET), 1995.

9. E. Greenspan, A. Schneider and A. Misolovin, "The Physics and Applications of Subcritical Light Water U-Pu Lattices," Proc. Topical Meeting on Advances in Reactor Physics, CONF-780401, Gatlinburg, TN., pp. 411-422 (1978).

10. K. Aoki, S. Kasai and S. Hattori, "Design of Small and Simple LMR Cores for Power Generation in Remote Communities," Proc. 3rd ASME-JSME Int. Conf. On Nuclear Engineering, ICONE-3, Tokyo, Japan, Oct. 1995.

11. S. Hattori and A. Minato, "A Large Modular LMR Power Station Which Meets Current Requirements," Proc. 3rd ASME-JSME Int. Conf. On Nuclear Engineering, ICONE-3, Tokyo, Japan, Oct. 1995.

12. E. Greenspan, H. Shimada, D.C. Wade, M.D. Carelli, L. Conway, N.W. Brown and Q. Hossain "The Encapsulated Nuclear Reactor Heat Source Reactor Concept," Proc. of 8th International Conference on Nuclear Engineering: ICONE 8, Paper 8750, Baltimore, MD, April 2-6, 2000.

13. J.F. Briesmeister, Ed., "MCNP – A General Monte Carlo N-Particle Transport Code", Los-Alamos National Laboratory Report LA-12625-M, Version 4B (1997).

14. A.G. Croff, "ORIGEN2 - A Revised and Updated Version of the Oak Ridge Code," Oak Ridge National Laboratory Report ORNL/TM-7175, 1980.

15. R. L. Moore at al.,"MOCUP:MCNP-ORIGEN2 Coupled Utility Program," Idaho National Engineering Laboratory Report INEL-95/0523, 1995.

16. K. Wang, Personal communication with Dr. C. Wemple of INEEL, 1999.

Table I. Zone Dimensions and Composition in ENHS Model of Fig. 1

No.	Item	Material (Volume Fraction)			Diameter	Height	Cold	Hot
		Lead	SS	Fuel	(cm)	(cm)	Temp.(K)	Temp.(K)
1	Safety rod region	0.99	0.01	-	10.67332	930	293	753
2	Lower shield	1.00	-	-	53.36822	100	293	693
3	Lower core support	-	1.00	-	53.36822	30	293	693
4	Core	0.31	0.21	0.48	53.36822	400	293	753
5	Fission gas plenum	0.31	0.21	-	53.36822	300	293	813
6	Upper shield	1.00	-	-	53.36822	100	293	813
7	Inner Pb gap	1.00	-	-	56.36822	930	293	753
8	Core barrel	-	1.00	-	57.36822	930	293	753
9	Outer Pb gap	1.00	-	-	58.36822	930	293	693
10	Reflector	1.00	-	-	73.36822	400	293	693
11	Cavity	-	0.10	-	73.36822	400	293	693
12	Upper cavity	0.90	0.10	-	73.36822	400	293	693
13	Reflector guide	0.70	0.30	-	75.36822	930	293	693
14	Down comer	1.00	-	-	82.36822	930	293	693
15	Sheild	1.00	-	-	126.8682	930	293	693
16	Vessel	-	1.00	-	127.8682	930	293	693

Table II. Actinides and Cross-Sections used for MCNP Calculations(Temp. in Kelvin)

Nuclides	**Cross Section Data**
For cold condtion	
^{234,235,236,238}U(293K)	92234.60c, 92235.60c, 92236.60c, 92238.60c
^{238,239,240,241,242}Pu(293K)	94238.60c, 94239.60c, 94240.60c, 94241.60c, 94242.60c
^{237}Np(293K)	93237.60c
^{241,243}Am(293K)	95241.60c, 95243.60c
^{242,243,244,245,246}Cm(293K)	96242.60c, 96243.60c, 96244.60c, 96245.60c, 96246.60c
For hot condtion	
^{234,235,236,238}U(755K)	92234.60c, 92235.60c, 92236.60c, 92238.60c
^{238,239,240,241,242}Pu(755K)	94238.60c, 94239.60c, 94240.60c, 94241.60c, 94242.60c

Table III. Fission Products and Cross-Sections used for MCNP Calculations (Temp. in K)

Nuclides	Cross Section Data
^{83,84,86}Kr(294K)	36083.59c, 36084.59c, 36086.59c
^{85,87}Rb(294K)	37085.55c, 37087.55c
^{90,91,92,93,94,96}Zr(600K)	40090.78c, 40091.78c, 40092.78c, 40093.78c, 40094.78c, 40096.78c
^{95}Mo(294K)	42095.50c
^{99}Tc(294K)	43099.60c
^{101}Ru(294K)	44101.50c
^{103}Rh(600K)	45103.78c
^{105,108}Pd(294K)	46105.50c 46108.50c
^{109}Ag(755K)	47109.84c
^{112,113}Cd(600K)	48112.78c, 48113.78c
^{127,129}I(600K)	53127.78c, 53129.78c
^{131,132,134,135,136}Xe(600K)	54131.78c, 54132.78c, 54134.78c, 54135.78c,
^{133,135,137}Cs(600K)	55133.78c, 55135.78c, 55137.78c
^{134,137,138}Ba(600K)	56134.78c, 56137.78c, 56138.78c
^{141}Pr(294K)	59141.50c
^{143,145}Nd(294K)	60143.50c, 60145.50c
^{147}Pm(294K)	61147.50c
^{147,149,150,151,152}Sm(294K)	62147.50c, 62149.50c, 62150.50c, 62151.50c,
^{153,154,155}Eu(294K)	63153.60c, 63154.50c, 63155.50c
^{155,156}Gd(755K)	64155.84c, 64156.84c

Table IV. Average Delayed Neutron Fraction for a 250MW, 4 m High Core of p/d=1.15 and q'av=120W/cm

	Fission Rate	Average ν	β value
^{235}U	0.005544	2.47	0.0068
^{238}U	0.058367	2.53	0.0158
^{239}Pu	0.229850	2.95	0.00215
^{240}Pu	0.017510	2.87	0.0031
^{241}Pu	0.027835	2.98	0.00515
^{242}Pu	0.002732	2.88	0.0072
Average			0.00461

Table V. Average Recoverable Energy in a 250MW, 4 m High Core of p/d=1.15 and q'av=120W/cm

	Recoverable energy[a] (MeV/fission)	Fission reaction rate from MCNP neutron balance
^{235}U	201.7	0.005281
^{238}U	202.8	0.058805
^{239}Pu	210.6	0.22802
^{240}Pu	211.0	0.017679
^{241}Pu	211.3	0.027358
^{242}Pu	211.7	0.002733
Average	209.2	

[a]Recoverable energy (MeV/fission) =0.00129927 $Z^2 A^{0.5}$ + 33.12[14], where Z and A are the atomic number and the atomic mass,

Table VI. Data for 250MWth Cores

Case Core height(m) p/d		4 1.15	4 1.30	4 1.45	4 1.60	2 1.15	2 1.30	2 1.45	2 1.60	1 1.15	1 1.30	1 1.45	1 1.60
Core thermal power	(MWth)	250	250	250	250	250	250	250	250	250	250	250	250
Average linear heat rate	(W/cm)	120	120	120	120	120	120	120	120	120	120	120	120
Net station efficiency	(%)	40	40	40	40	40	40	40	40	40	40	40	40
Core height	(cm)	400	400	400	400	200	200	200	200	100	100	100	100
Fission gas plenum length	(cm)	300	300	300	300	150	150	150	150	75	75	75	75
Core diameter	(cm)	106.8	120.6	134.6	148.6	149.4	169	188.4	208	210.2	237.6	265	292.6
Vessel diameter	(cm)	255.8	269.6	283.6	297.6	298.4	318	337.4	357	359.2	386.6	414	441.6
Core inlet temp.	(K)	753	753	753	753	753	753	753	753	753	753	753	753
Core outlet temp.	(K)	813	813	813	813	813	813	813	813	813	813	813	813
No. fuel assemblies		24	24	24	24	48	48	48	48	96	96	96	96
No. shutdown assemblies		1	1	1	1	1	1	1	1	1	1	1	1
Pu enrichment*	(wt%)	10.994	11.797	12.709	13.557	10.000	10.820	11.664	12.553	10.173	11.188	12.243	13.375
No. fuel rods/assembly		217	217	217	217	217	217	217	217	217	217	217	217
Fuel rod outer diameter	(cm)	1.2	1.2	1.2	1.2	1.2	1.2	1.2	1.2	1.2	1.2	1.2	1.2
Clad thickness	(cm)	0.1	0.1	0.1	0.1	0.1	0.1	0.1	0.1	0.1	0.1	0.1	0.1
Fuel rod pitch/diameter		1.15	1.3	1.45	1.6	1.15	1.3	1.45	1.6	1.15	1.3	1.45	1.6
Fuel material		Pu-U-Zr	Pu-U-Zr	Pu-U-Zr	Pu-U-Zr	Pu-U-Zr	Pu-U-Zr	Pu-U-Zr	Pu-U-Zr	Pu-U-Zr	Pu-U-Zr	Pu-U-Zr	Pu-U-Zr
Clad material		SUS	SUS	SUS	SUS	SUS	SUS	SUS	SUS	SUS	SUS	SUS	SUS
Result													
Initial Conversion Ratio(ICR)@Cold		1.162944	1.103999	1.039082	0.990175	1.294979	1.218041	1.147972	1.083373	1.265015	1.164482	1.081527	1.002335
Reflector reactivity worth	(dk)	0.02319	0.02375	0.02347	0.021	0.01363	0.01635	0.01258	0.01011	0.00341	0.00747	0.0038	0.00595
Void reactivity	(dk)	0.01938	0.02802	0.04012	0.04476	0.02208	0.03118	0.0393	0.04343	0.01867	0.02552	0.03035	0.03231
Hot to cold reactivity swing**	(dk)	-0.00466	-0.00175	-0.00227	-0.00015	-0.00464	-0.00342	-0.00016	0.00061	-0.00148	-0.00299	0.00143	-0.00199
All coolant loss reactivity swing	(dk)	-0.12939	-0.15316	-0.17967	-0.21013	-0.05811	-0.07628	-0.10187	-0.12741	-0.03734	-0.05813	-0.08949	-0.11702
BOC fuel material													
^{235}U	(t)	0.031162	0.030881	0.030562	0.030265	0.03151	0.031223	0.030927	0.030616	0.03145	0.031094	0.030725	0.030328
^{238}U	(t)	15.54996	15.40965	15.25027	15.10217	15.72355	15.58031	15.43285	15.2776	15.69339	15.51598	15.33176	15.13387
^{239}Pu	(t)	1.293271	1.387765	1.495103	1.594845	1.176375	1.272838	1.372156	1.476684	1.196718	1.31616	1.440227	1.573458
^{240}Pu	(t)	0.417621	0.448132	0.482794	0.515002	0.379871	0.411021	0.443091	0.476846	0.38644	0.425009	0.465073	0.508098
^{241}Pu	(t)	0.123169	0.132168	0.142391	0.15189	0.112036	0.121223	0.130682	0.140637	0.113973	0.125348	0.137165	0.149853
^{242}Pu	(t)	0.090452	0.097061	0.104568	0.111544	0.082276	0.089023	0.095969	0.10328	0.083699	0.092053	0.10073	0.110048
Total	(t)	17.50564	17.50565	17.50568	17.50572	17.50562	17.50564	17.50567	17.50566	17.50567	17.50564	17.50567	17.50565
With reflector													
Peak-to-average radial flux factor		1.28	N/A	N/A	1.32	1.37	N/A	N/A	N/A	N/A	N/A	N/A	N/A
Peak-to-average axial flux factor		1.43	N/A	N/A	1.41	1.35	N/A	N/A	N/A	N/A	N/A	N/A	N/A

* Pu/(U+Pu)

** Material expansion is neglected except for that of coolant

Table VII. Data for 125MWth cores

Case Core height(m) p/d		4 1.15	4 1.3	4 1.45	4 1.6	2 1.15	2 1.3	2 1.45	2 1.6	1 1.15	1 1.3	1 1.45	1 1.6
Core thermal power	(MWth)	125	125	125	125	125	125	125	125	125	125	125	125
Average linear heat rate	(W/cm)	120	120	120	120	120	120	120	120	120	120	120	120
Net station efficiency	(%)	40	40	40	40	40	40	40	40	40	40	40	40
Core height	(cm)	400	400	400	400	200	200	200	200	100	100	100	100
Fission gas plenum length	(cm)	300	300	300	300	150	150	150	150	75	75	75	75
Core diameter	(cm)	77	87	97	107	106.8	120.6	134.6	148.6	149.4	169	188.4	208
Vessel diameter	(cm)	226	236	246	256	255.8	269.6	283.6	297.6	298.4	318	337.4	357
Core inlet temp.	(K)	753	753	753	753	753	753	753	753	753	753	753	753
Core outlet temp.	(K)	813	813	813	813	813	813	813	813	813	813	813	813
No. fuel assemblies		12	12	12	12	24	24	24	24	48	48	48	48
No. shutdown assemblies		1	1	1	1	1	1	1	1	1	1	1	1
Pu enrichment*	(wt%)	13.59522	14.65678	15.77822	16.73567	11.53811	12.46244	13.45733	14.44044	11.14356	12.25389	13.4000	14.62367
No. fuel rods/assembly		217	217	217	217	217	217	217	217	217	217	217	217
Fuel rod outer diameter	(cm)	1.2	1.2	1.2	1.2	1.2	1.2	1.2	1.2	1.2	1.2	1.2	1.2
Clad thickness	(cm)	0.1	0.1	0.1	0.1	0.1	0.1	0.1	0.1	0.1	0.1	0.1	0.1
Fuel rod pitch/diameter		1.15	1.3	1.45	1.6	1.15	1.3	1.45	1.6	1.15	1.3	1.45	1.6
Fuel material		Pu-U-Zr	Pu-U-Zr	Pu-U-Zr	Pu-U-Zr	Pu-U-Zr	Pu-U-Zr	Pu-U-Zr	Pu-U-Zr	Pu-U-Zr	Pu-U-Zr	Pu-U-Zr	Pu-U-Zr
Clad material		SUS	SUS	SUS	SUS	SUS	SUS	SUS	SUS	SUS	SUS	SUS	SUS
Result													
Initial Conversion Ratio(ICR)@Cold		0.900343	0.84931	0.801681	0.769016	1.092047	1.026838	0.967191	0.91334	1.13546	1.043783	0.969303	0.896342
Reflector reactivity worth	(dk)	0.04402	0.04395	0.04479	0.04341	0.02426	0.02315	0.02505	0.02379	0.01126	0.01484	0.01114	0.01327
Void reactivity	(dk)	0.00903	0.01359	0.01748	0.02172	0.0133	0.01885	0.0235	0.02473	0.01174	0.01382	0.01391	0.01398
Hot to cold reactivity swing**	(dk)	-0.00873	-0.00681	-0.00475	-0.0088	-0.0033	-0.00345	-0.0066	-0.00533	-0.00352	-0.00753	-0.0039	-0.00432
BOC fuel material													
^{235}U	(t)	0.015126	0.01494	0.014744	0.014576	0.015486	0.015324	0.01515	0.014978	0.015555	0.015361	0.01516	0.014946
^{238}U	(t)	7.547755	7.455009	7.357024	7.273411	7.727449	7.646691	7.559781	7.473909	7.76186	7.66491	7.564796	7.457906
^{239}Pu	(t)	0.79966	0.862098	0.928056	0.984374	0.678661	0.733029	0.791548	0.849373	0.655452	0.720763	0.78818	0.86015
^{240}Pu	(t)	0.258222	0.278386	0.299685	0.317872	0.219151	0.236707	0.255604	0.274277	0.211656	0.232746	0.254516	0.277757
^{241}Pu	(t)	0.076158	0.082104	0.088386	0.09375	0.064634	0.069812	0.075385	0.080893	0.062424	0.068644	0.075065	0.081919
^{242}Pu	(t)	0.055929	0.060295	0.064909	0.068848	0.047466	0.051268	0.055361	0.059406	0.045843	0.050411	0.055125	0.060159
Total	(t)	8.752849	8.752832	8.752803	8.752831	8.752847	8.752832	8.752829	8.752836	8.75279	8.752834	8.752842	8.752837
With reflector													
Peak-to-average radial flux factor		N/A	N/A	N/A	N/A	1.29	N/A	N/A	N/A	1.4	N/A	N/A	N/A
Peak-to-average axial flux factor		N/A	N/A	N/A	N/A	1.36	N/A	N/A	N/A	1.23	N/A	N/A	N/A

* Pu/(U+Pu)

** Material expansion is neglected except for that of coolant

Table VIII. Change in keff due to Pb Level Drop from in the Reactor Vessel.
2m High Core of 250MWth and 120 W/cm Average Linear Heat Rate.
Reference Pb Level is 4.5 m above Core Bottom

Pb Level	p/d			
from core bottom(m)	1.15	1.30	1.45	1.60
2.75	0.00006	0.00255	-0.00088	-0.00405
2.0 (core top)	-0.00265	-0.00279	-0.00945	-0.01298
1.0	-0.03341	-0.03741	-0.05346	-0.06376
0.0	-0.05625	-0.07101	-0.09436	-0.11884

Table IX. Hot-to-Cold Reactivity Swing for Selected Cores

Total thermal power(MWth) **Case Core height(m) + p/d** **ALHGR(W/cm)**	**250** **4+1.30** **120**	**250** **2+1.525** **120**	**125** **1+1.15** **120**	**250** **4+1.55** **80**	**125** **2+1.30** **80**
Hot to cold reactivity swing(dT=460K) (dk)	-0.01307	-0.00781	-0.01215	-0.00957	-0.00768
Hot to cold reactivity swing(dT=130K) (dk)	-0.00469	-0.00374	-0.00459	-0.00379	-0.00314

Table X. Evolution of Inventory of Fuel Isotopes in the 125MW_{th}, 2m High Core Designed with p/d=1.30 and q'_{av}=80W/cm

	YEAR						
	0	5	10	15	20	25	30
^{235}U	0.023261	0.019242	0.015963	0.01329	0.011104	0.009316	0.007856
^{238}U	11.60731	11.32986	11.05919	10.79629	10.53989	10.28944	10.04469
^{239}Pu	1.007076	1.049243	1.07846	1.097299	1.108009	1.112101	1.110856
^{240}Pu	0.325201	0.332238	0.339489	0.34669	0.353678	0.360402	0.366546
^{241}Pu	0.095912	0.068625	0.051958	0.041839	0.03574	0.032145	0.030096
^{242}Pu	0.070435	0.069167	0.067579	0.065848	0.064061	0.062287	0.060548
^{234}U	1.28E-21	1.15E-05	7.84E-05	0.000228	0.000462	0.000774	0.00115
^{236}U	1.29E-21	0.000985	0.00179	0.002449	0.002993	0.003445	0.003821
^{238}Pu	1.3E-21	0.000807	0.002855	0.005385	0.007984	0.010445	0.012663
^{241}Am	1.32E-21	0.018059	0.02877	0.035067	0.038725	0.040815	0.041998
^{243}Am	1.33E-21	0.002098	0.003882	0.005391	0.006677	0.007757	0.008659
^{237}Np	1.3E-21	0.001027	0.002022	0.002952	0.003784	0.00452	0.005166
^{242}Cm	1.32E-21	0.000208	0.00035	0.000436	0.000484	0.000509	0.000526
^{243}Cm	1.33E-21	1.69E-06	5.7E-06	1.02E-05	1.42E-05	1.76E-05	2.03E-05
^{244}Cm	1.33E-21	0.000103	0.000352	0.000682	0.001048	0.001422	0.001784
^{245}Cm	1.34E-21	2.14E-06	1.44E-05	4.09E-05	8.18E-05	0.000136	0.0002
^{246}Cm	1.35E-21	1.29E-08	1.77E-07	7.71E-07	2.11E-06	4.46E-06	8.05E-06

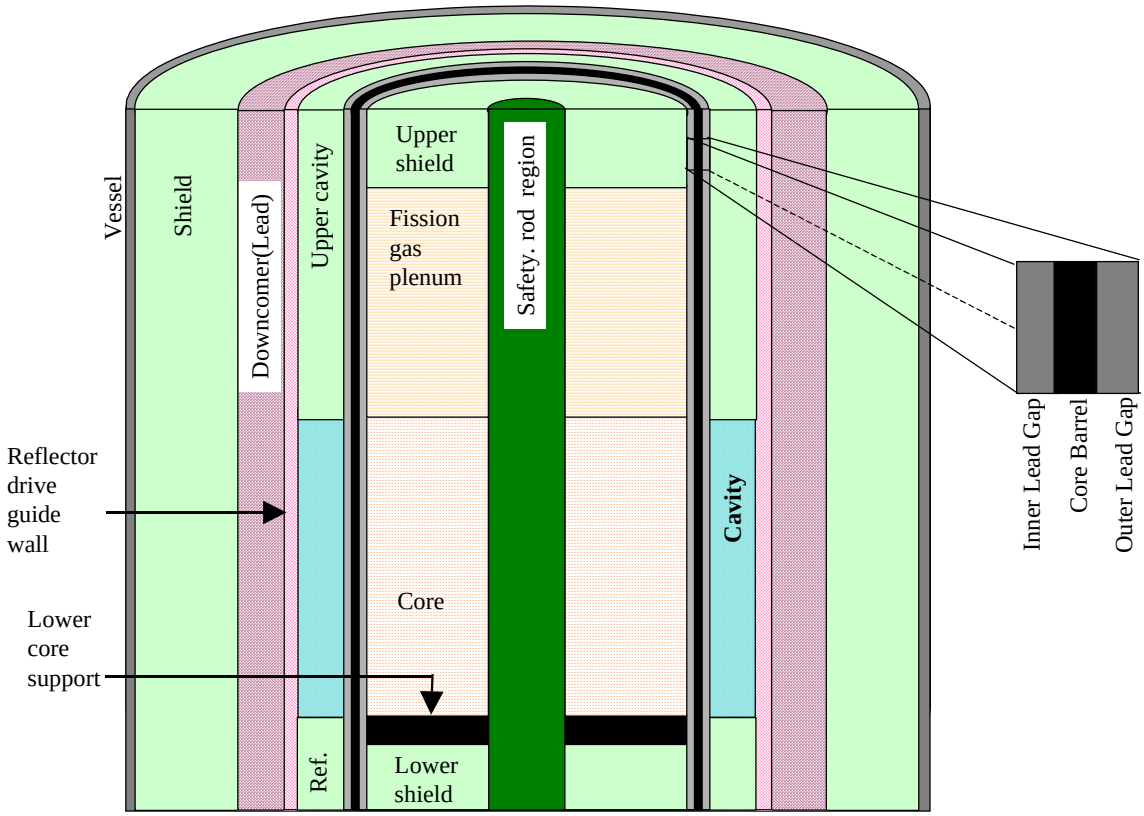

Figure 1. ENHS Core Layout; Vertical Cut

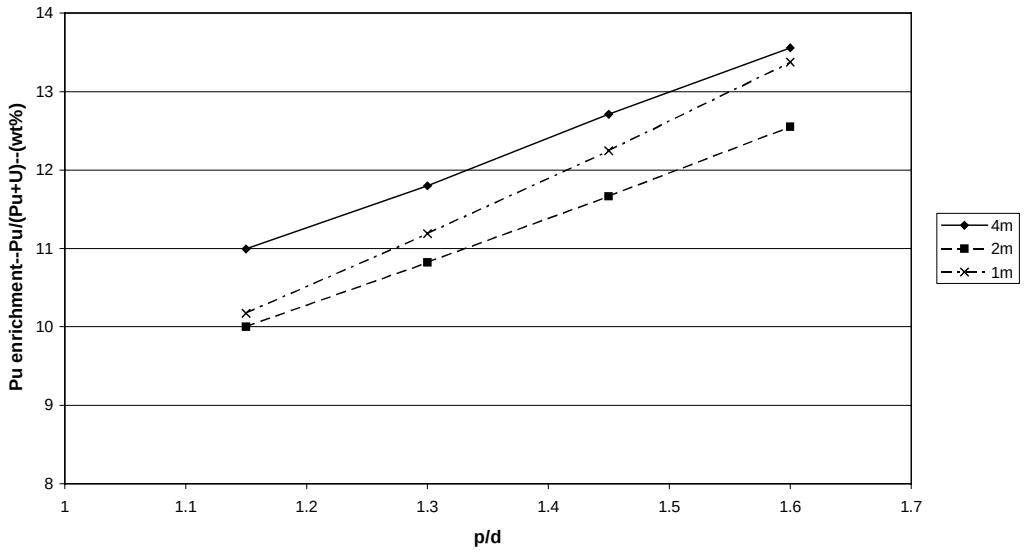

Figure 2. Dependence of Critical Pu Concentration on Lattice p/d and Core Height

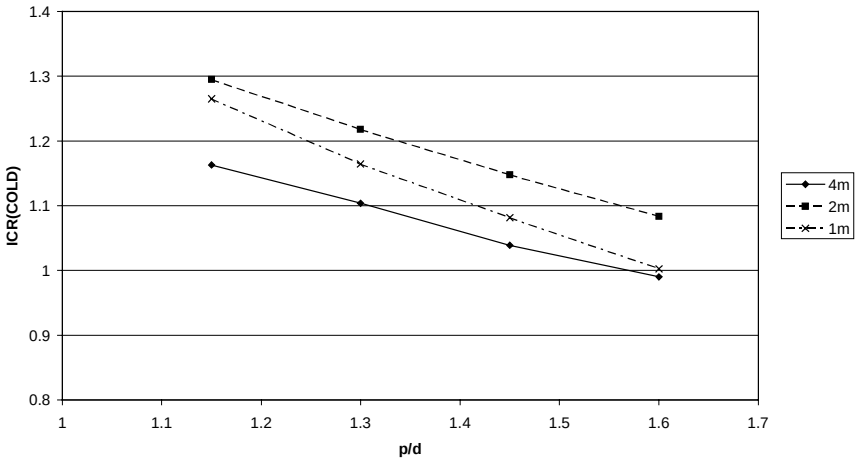

Figure 3. Dependence of ICR on Lattice p/d and Core Height

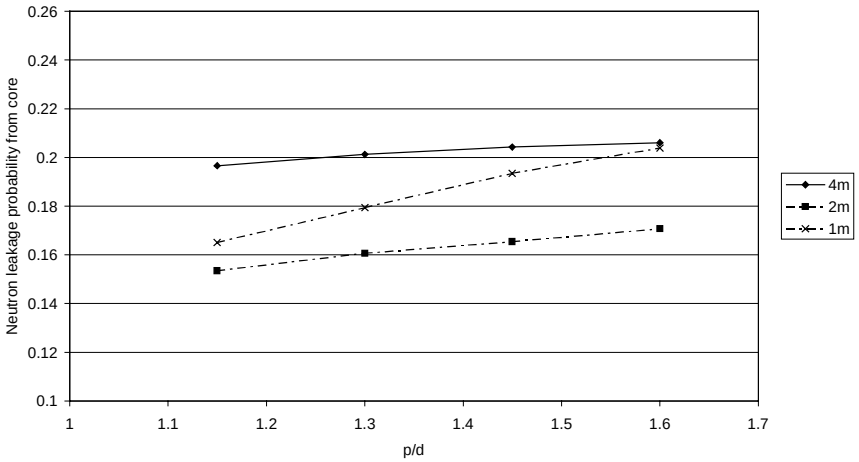

Figure 4. Dependence of Leakage Probability on Lattice p/d and Core Height

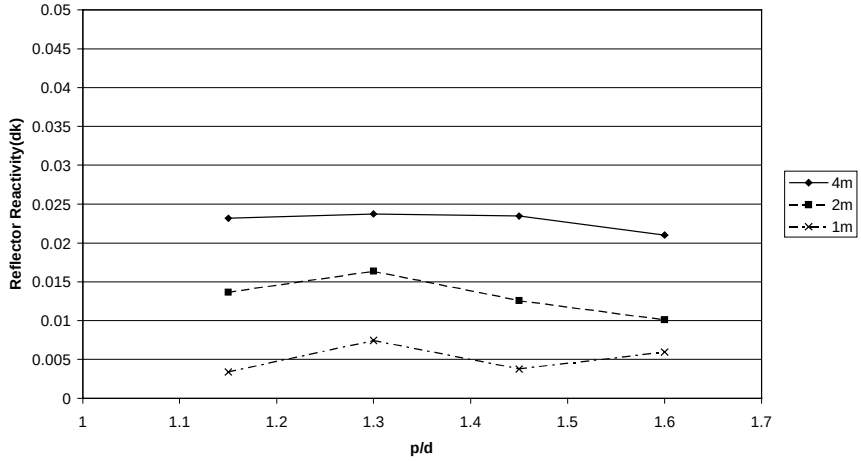

Figure 5. Dependence of Reflector Reactivity Worth on Lattice p/d and Core Height

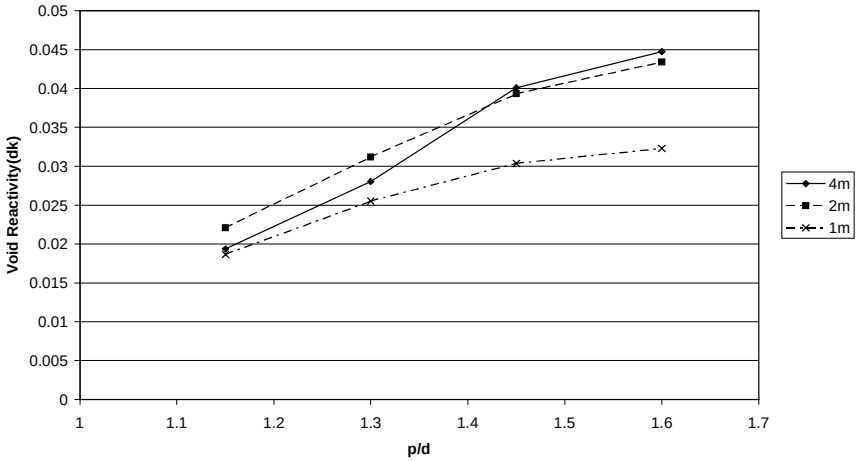

Figure 6. Dependence of Void Reactivity on Lattice p/d and Core Height

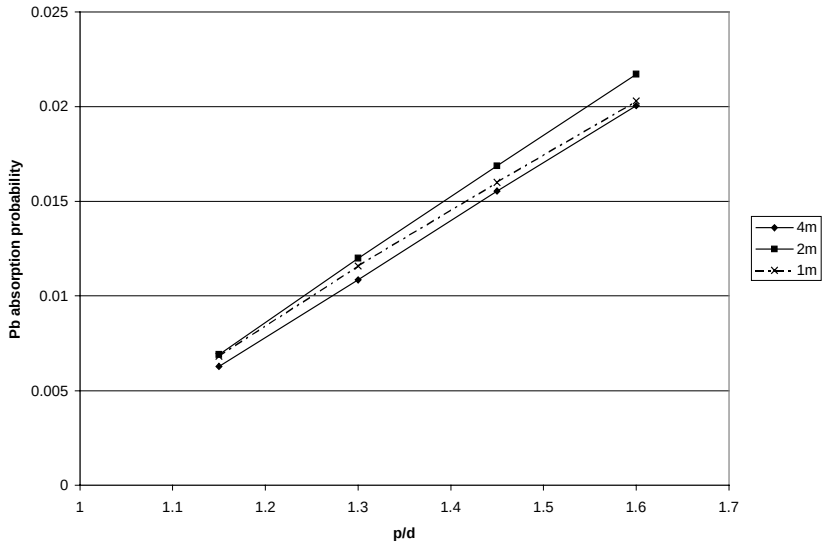

Figure 7. Dependence of Absorption Probability in Pb on Lattice p/d and Core Height

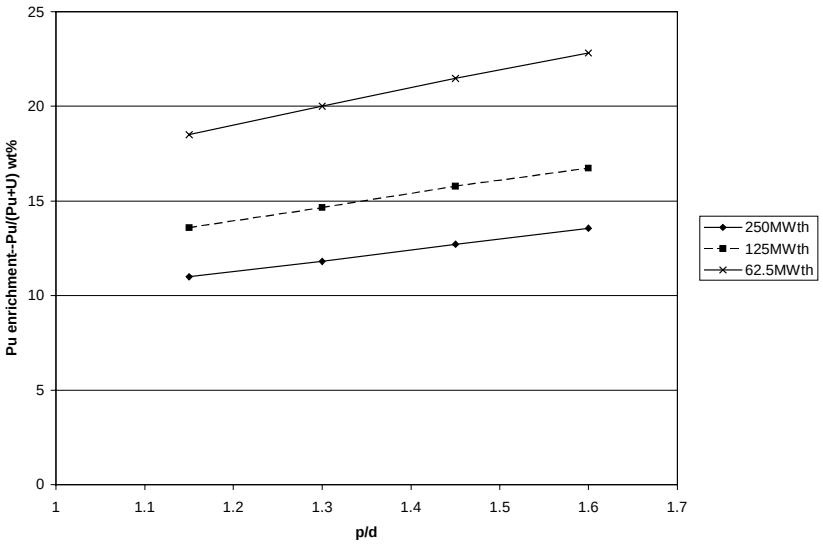

Figure 8. Dependence of Critical Pu Concentration on Lattice p/d and Core Power for 4m High Cores

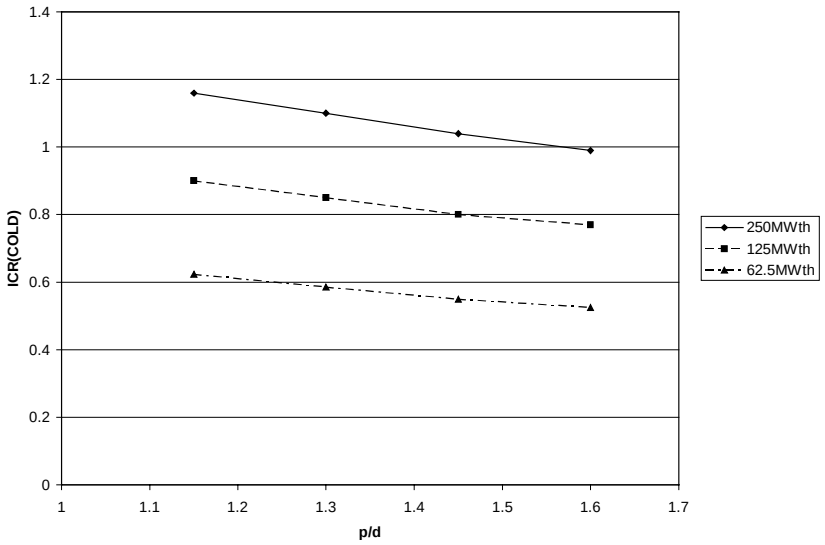

Figure 9. Dependence of ICR on Lattice p/d and Core Power for 4m High Cores

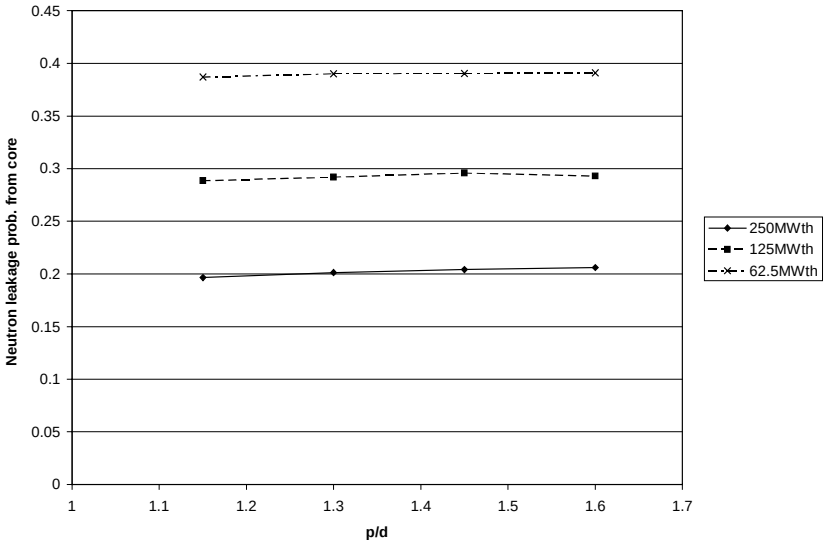

Figure 10. Dependence of Leakage probability on Lattice p/d and Core Power for 4m High Cores

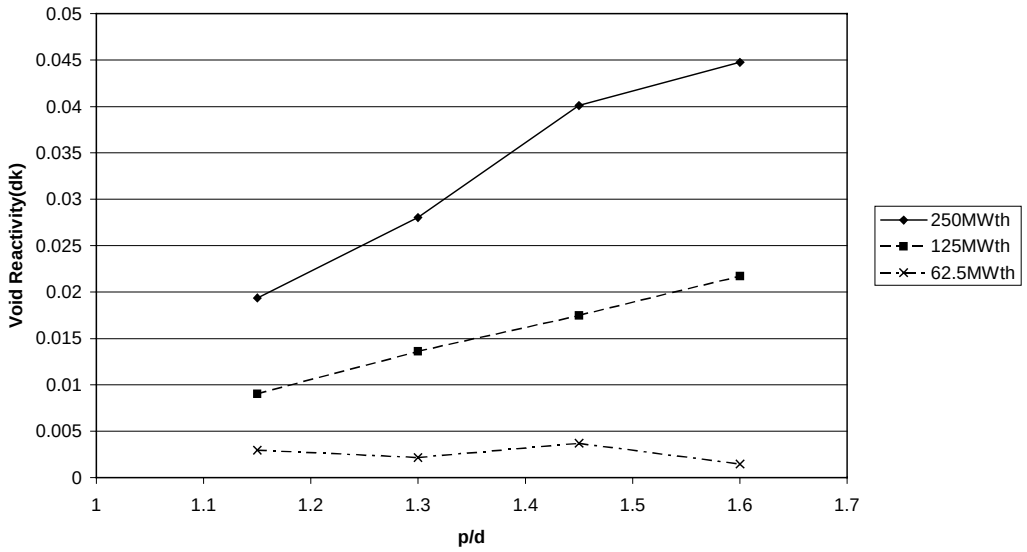

Figure 11. Dependence of Reflector Reactivity Worth on Lattice p/d and Core Power for 4m High Cores

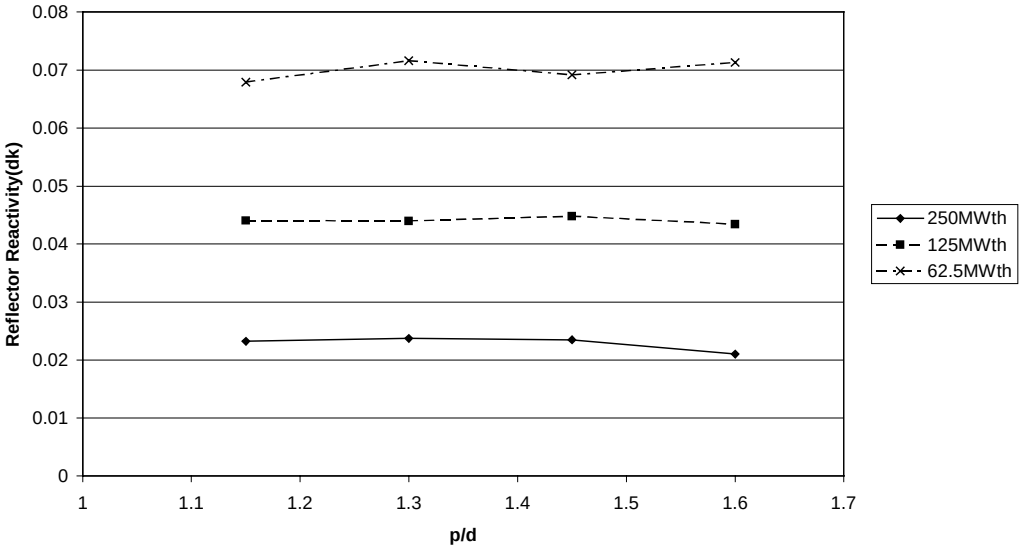

Figure 12. Dependence of Void Reactivity on Lattice p/d and Core Power for 4m High Cores

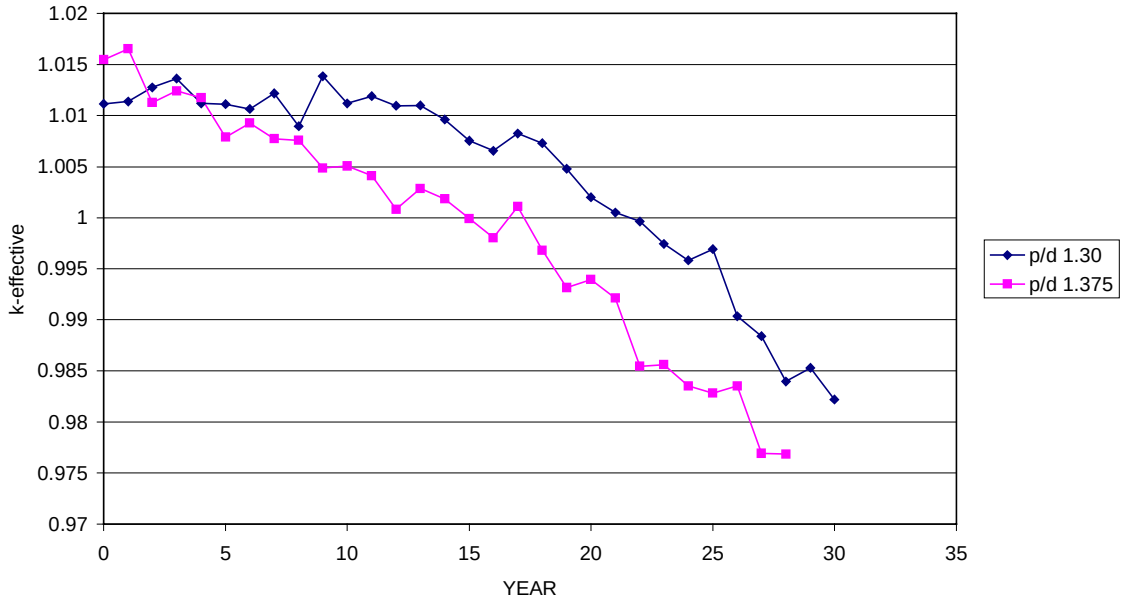

Figure 13. Variation of k_{eff} with Effective Full Power Years of 4m High Cores for 250MWth having q'_{av} of 120 W/cm

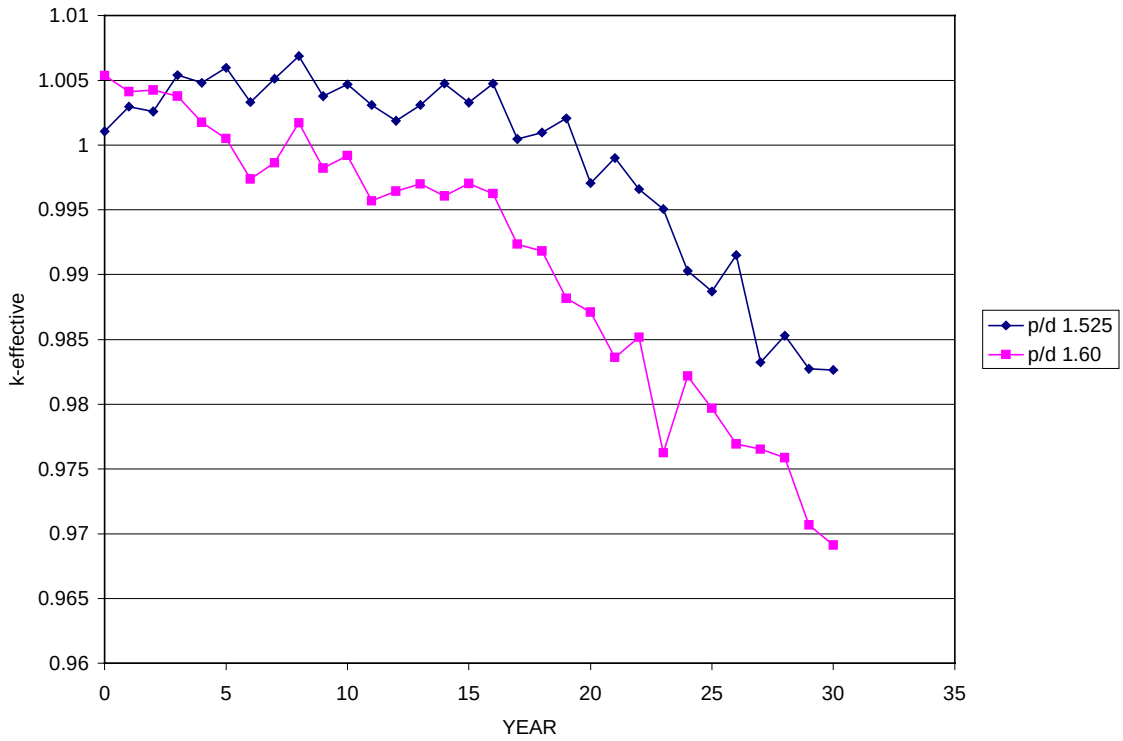

Figure 14. Variation of k_{eff} with Effective Full Power Years of 2m High Cores for 250MWth having q'_{av} of 120 W/cm

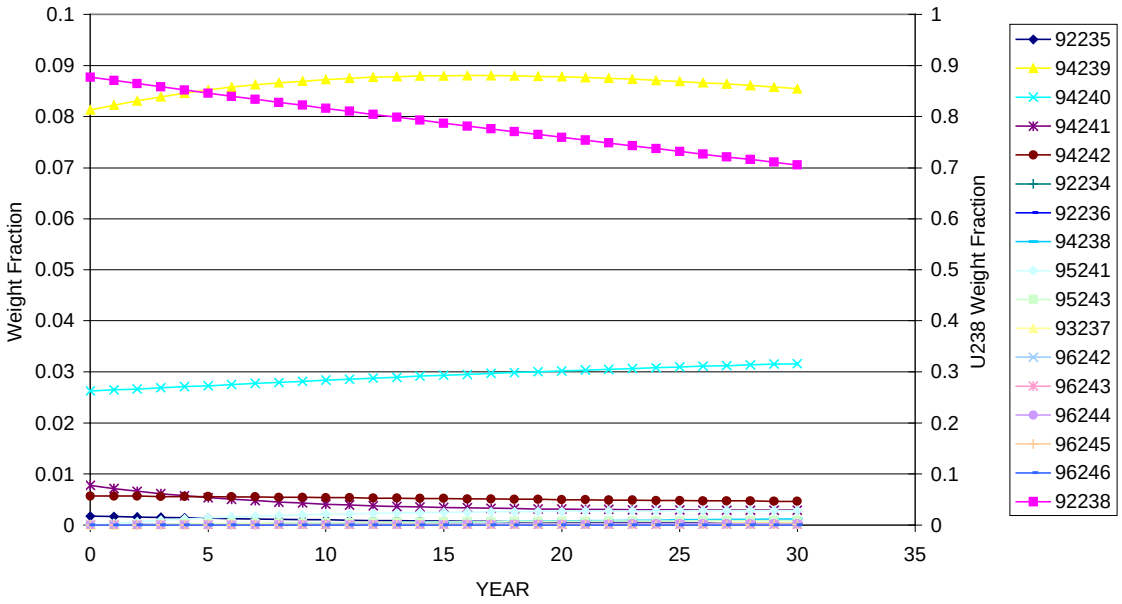

Figure 15. Evolution of Fuel Isotope Concentration with Effective Full Power Years of the p/d = 1.525 Core of Figure 14

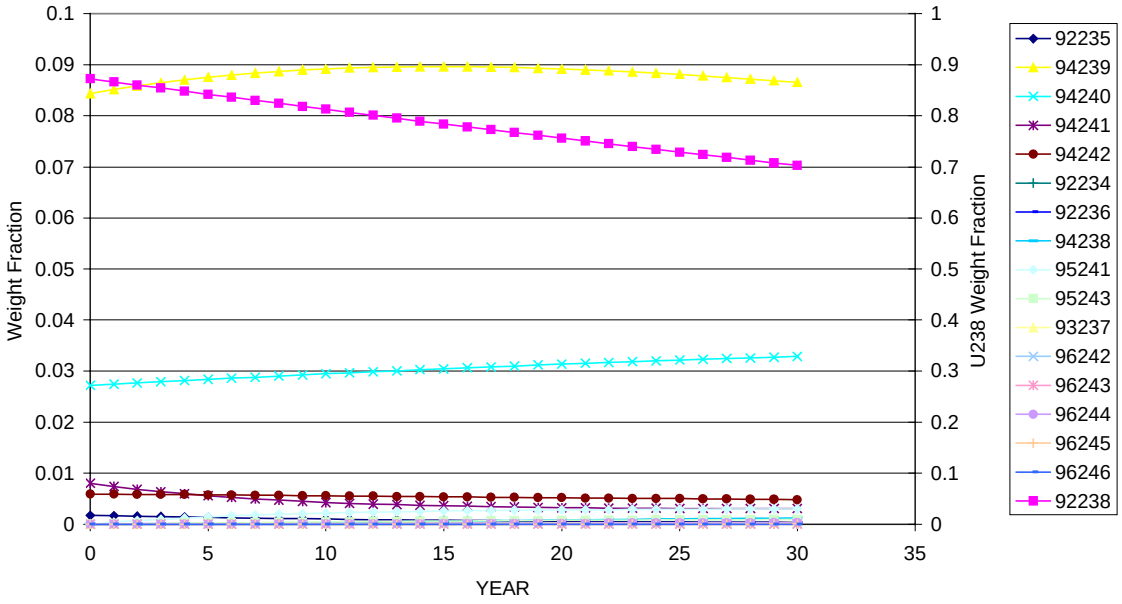

Figure 16. Evolution of Fuel Isotope Concentration with Effective Full Power Years of the p/d = 1.60 Core of Figure 14

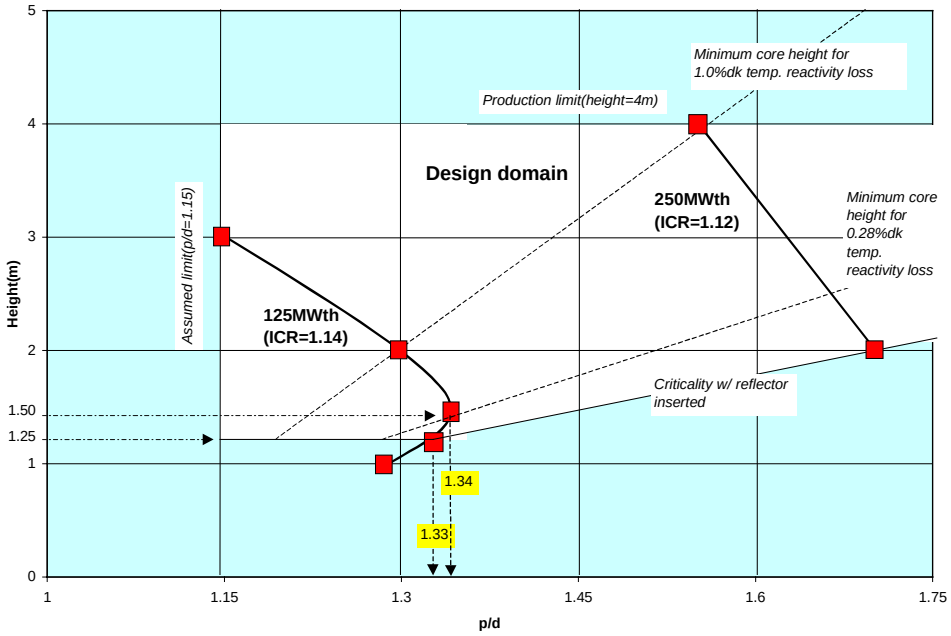

Figure 17. Design Domain of 80 W/cm Cores for ENHS Featuring Nearly Zero Burnup Reactivity Swing. Peak Fluence Constraint Limits Life to ~ 15EFPY

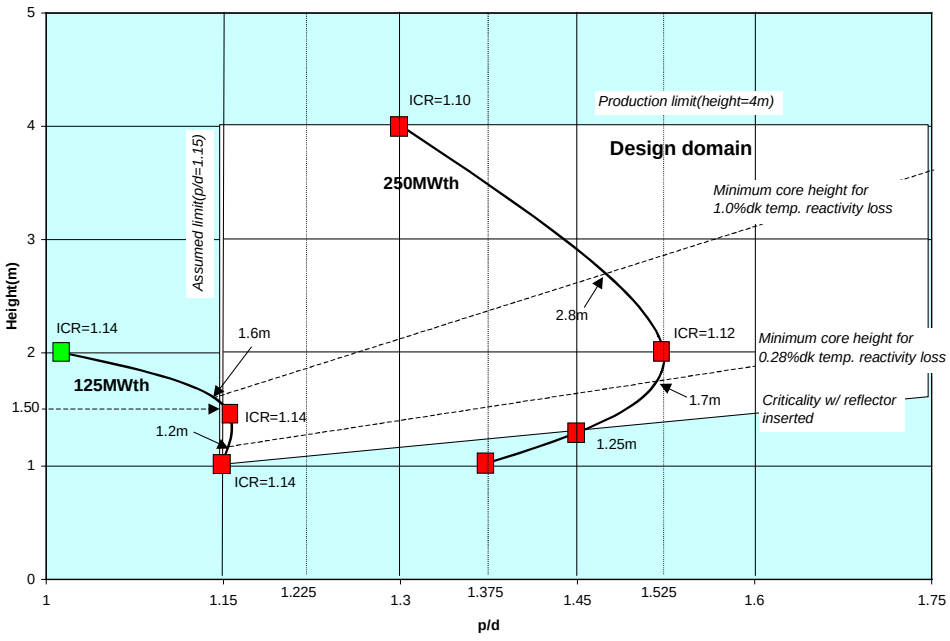

Figure 18. Design Domain of 120 W/cm Cores for ENHS Featuring Nearly Zero Burnup Reactivity Swing. Peak Fluence Constraint Limits Life to ~ 15EFPY

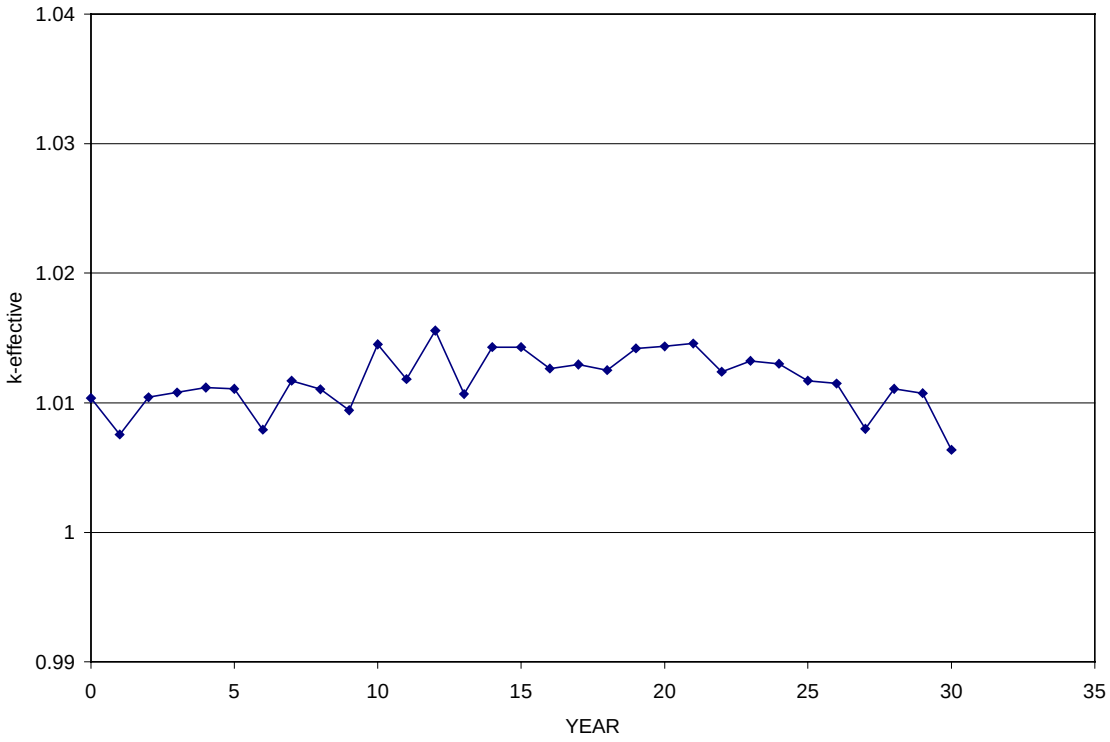

Figure 19. Variation of k_{eff} with Effective Full Power Years of a 2m High Core for $125MW_{th}$ having q'_{av} of 80W/cm and p/d of 1.30

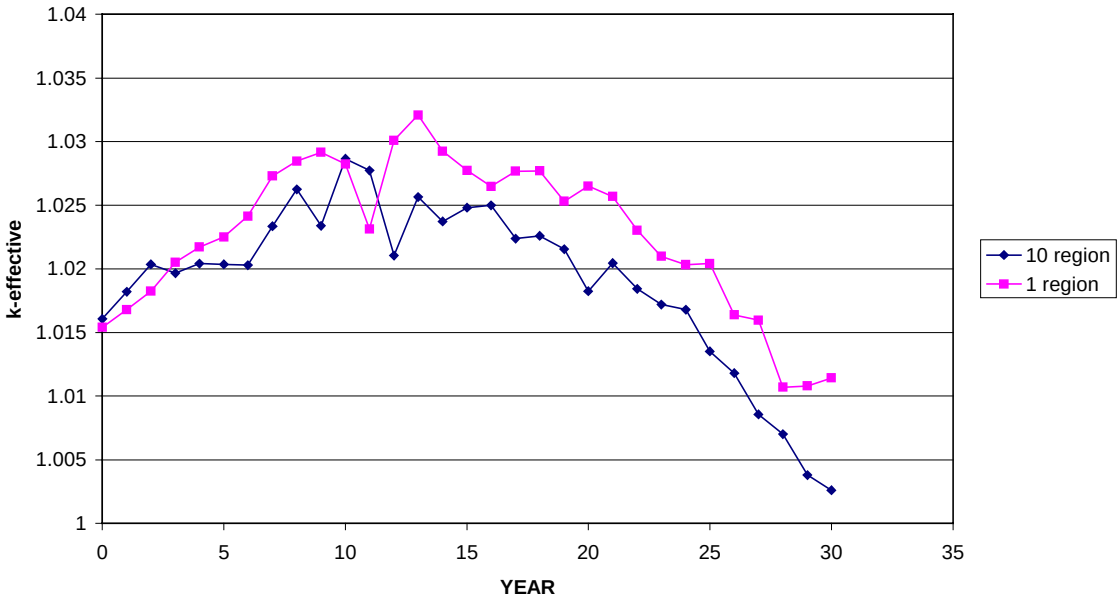

Figure 20. Effect of Space Dependent Burnup on k_{eff} Evolution. Core is 4m High with p/d=1.15 and q'_{av}=120W/cm Operating at $250MW_{th}$

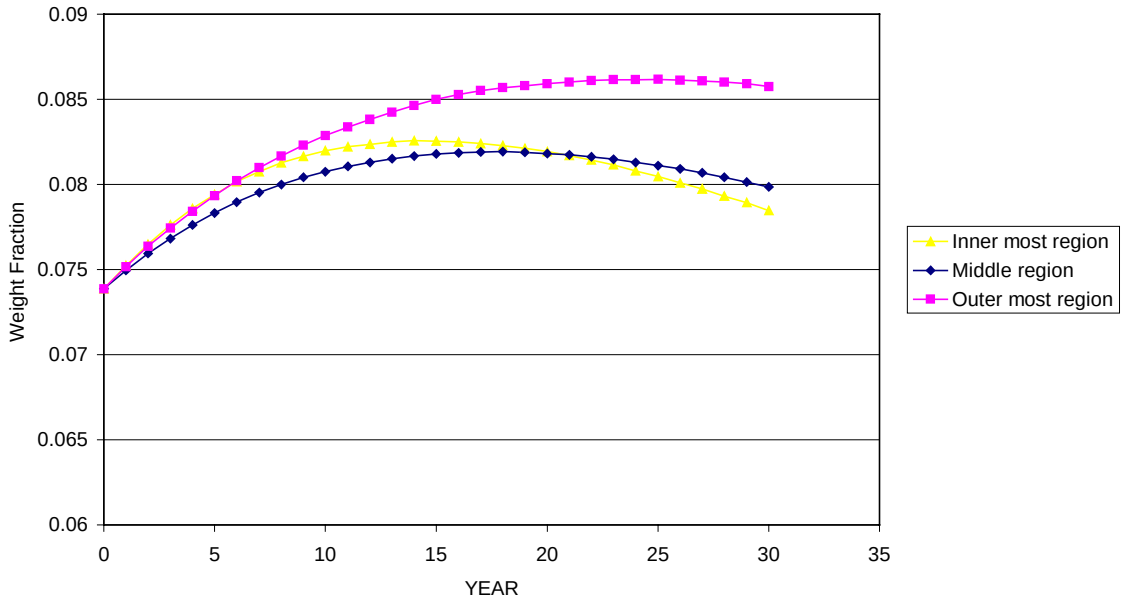

Figure 21. Effect of Space Dependent Burnup on ^{239}Pu Evolution. Core is 4m High with p/d=1.15 and q'_{av} =120 W/cm Operating at 250MW_{th}.

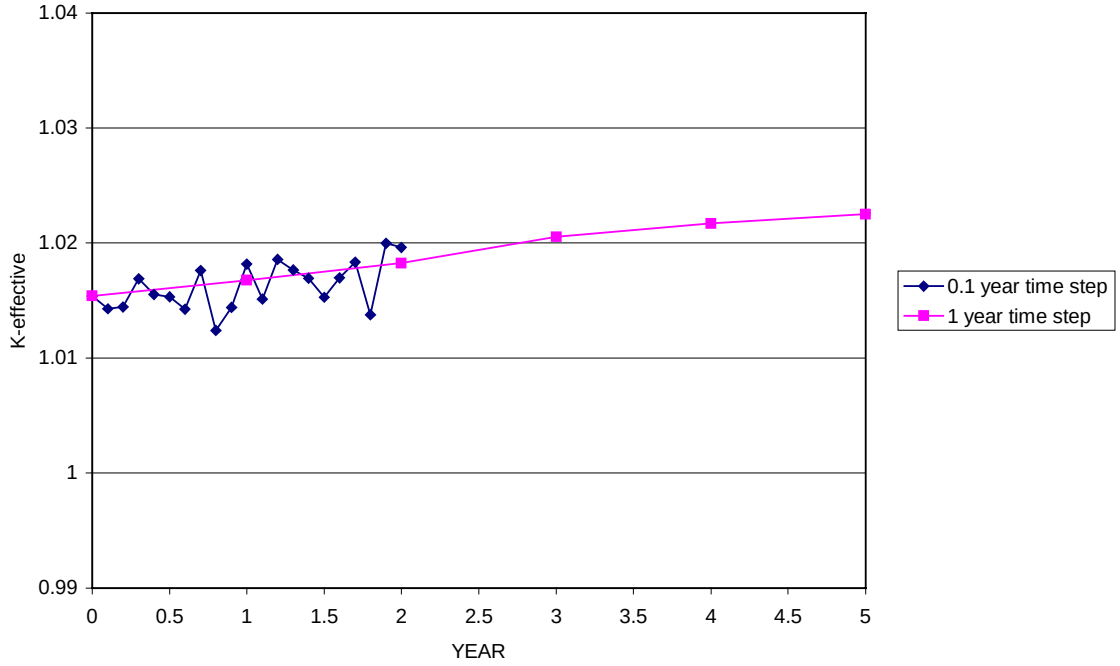

Figure 22. Effect of MCNP Calculation Frequency on k_{eff} Evolution. Core is 4m High with p/d=1.15 and q'_{av} =120 W/cm Operating at 250MW_{th}.

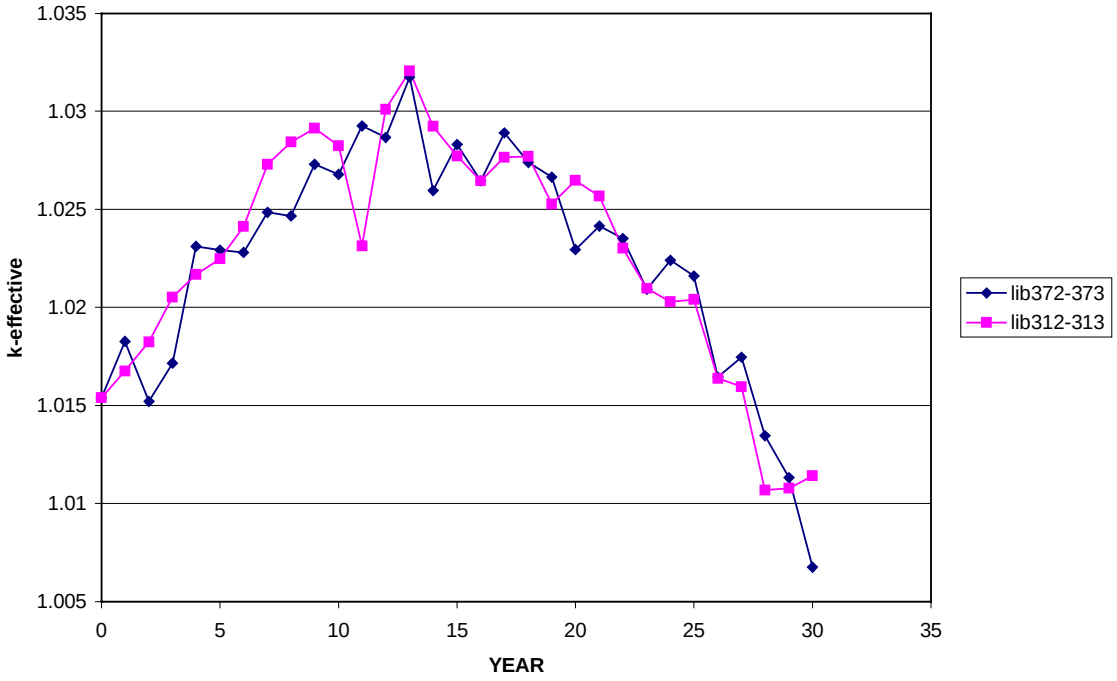

Figure 23. Effect of ORIGEN2 FP Library on k_{eff} Evolution. Core is 4m High with p/d=1.15 and q'_{av} =120 W/cm Operating at 250MW_{th}.